Robotica (2010) volume 28, pp. 737–745. © Cambridge University Press 2009
doi:10.1017/S0263574709990439

Design and similarity evaluation on humanoid motion based on human motion capture

Qiang Huang*, Zhangguo Yu, Weimin Zhang, Wei Xu and Xuechao Chen

Intelligent Robotics Institute, School of Mechatronical Engineering, Beijing Institute of Technology, 5 Nandajie, Zhongguancun, Haidian, Beijing, China

(Received in Final Form: July 29, 2009. First published online: August 28, 2009)

SUMMARY

This paper explores the design of humanoid complicated dynamic motion based on human motion capture. Captured human data must be adapted for the humanoid robot because its kinematics and dynamics mechanisms differ from those of the human actor. It is expected that humanoid movements are highly similar to those of the human actor. First, the kinematics constraints, including ground contact conditions, are formulated. Second, the similarity evaluation on the humanoid motion based on both the spatial and temporal factors compared with the human motion is proposed. Third, the method to obtain humanoid motion with high similarity is presented. Finally, the effectiveness of the proposed method is confirmed by simulations and experiments of our developed humanoid robot "sword" motion performance.

KEYWORDS: Humanoid robot; Similarity evaluation; Motion capture; Dynamic stability; Kinematics constraint.

1. Introduction

Many researchers have studied walking pattern generation for humanoid robots.[1–10] Basically, their methods start from the viewpoint of analytic equations. The advantage of such methods is that the necessary constraints of mechanisms, kinematics, and dynamics can be formulated first. Then, the humanoid motion satisfying the necessary humanoid constraints can be obtained by solving the formulated equations. However, in the case of complicated motions, such as human dance and sports performance, exact motion equations are difficult to formulate and solve.

Recently, some researchers have discussed the generation of complicated humanoid motion based on human motion capture.[11–16] Since the kinematics and dynamics mechanisms of the humanoid motion differ from those of the human actor, the captured trajectories must be modified to satisfy the constraints of kinematics and dynamics. Pollard *et al.*[11] demonstrated the dance motion of humanoid upper arms by capturing human dance. But this study did not investigate the stability of the robot. To obtain the humanoid motion taking the stability into consideration, Yamane *et al.*[12] presented the dynamics simulation of humanoid motion based on captured data. Nakaoka *et al.*[13,14] described a method using a symbolic description of leg motion primitives to create the real humanoid dance. Nakazawa *et al.*[15,16] presented a better method for matching the frames of human motions and created blended motions according to the matching result.[15,16]

The human trajectory is considered as a teaching motion. It is therefore accepted that the humanoid movements are highly similar to those of the human actor. The above mentioned investigations discussed how to obtain the humanoid motion based on human motion capture. However, how to evaluate the similarity of the humanoid motion comparing with the motion of the human actor quantitatively has not been studied sufficiently. In addition, most of the above mentioned investigations based on human motion capture discussed humanoid motion in the case of a relatively low speed.

This paper explores to propose a similarity function to evaluate the similarity of the humanoid motion compared with the human motion quantitatively based on both the spatial and temporal factors, and to design the humanoid complicated dynamic motion with similarity, kinematics constraints and dynamic stability in consideration. The structure of this paper is as follows. In Section 2, the procedure for designing humanoid motion is introduced. The kinematics constraints are formulated in Section 3. In Section 4, similarity evaluation function is proposed. In Section 5, the algorithm to derive the humanoid motion with high similarity and high stability is presented. Simulations and experiments are provided in Section 6, followed by the conclusions in Section 7.

2. Scheme of Motion Design

2.1. Model of the humanoid robot

We have developed a humanoid robot, BHR-02 (Fig. 1), 1.6 (m), 63 (kg), with 32 degrees of freedom (DOF) in total. For each leg, there are 3 DOF in the hip joint, 1 DOF in the knee joint, and 2 DOF in the ankle joint. For each arm, there are 3 DOF in the shoulder joint, 1 DOF in the elbow joint,

* Corresponding author. E-mail: qhuang@bit.edu.cn

(a) Humanoid and its model (b) Human and his model

Fig. 1. Human and humanoid model.

2 DOF in the wrist joint, and 3 DOF in the hand joint. For the head, there are 2 DOF.

Moreover, it is difficult to build an exact human dynamics model since human skeleton is very complicated.[17] In order to use the captured human trajectory to design the humanoid motion, a simplified human model with a rigid body-link is built (Fig. 1b), and the joints and the DOF of the human model are the same to those of the humanoid model (Fig. 1a).

2.2. *Procedure for humanoid motion design*

The procedure for generating humanoid motion from a human actor includes the following steps (Fig. 2):

(i) Human motion capture;
(ii) Segmentation of primitive motion;
(iii) Kinematics mapping;
(iv) Dynamics mapping;
(v) Similarity evaluation;
(vi) Simulation and experiment.

Our motion capture system consists of 12 optical cameras and 38 reverberation markers located on the actor's body. The system records the positions of all markers at the rate of 100 fps. The data of joint angles of the simplified human model is computed through kinematics based on the data captured by the motion capture system and the data is regarded as the actor's data which will be used in the following kinematics mapping and similarity evaluation.

The actor's data cannot be directly imported into the humanoid robot because its kinematics and dynamics mechanisms differ from those of the human actor's.

By using kinematics mapping, the actor's data is translated into the humanoid data, satisfying the humanoid kinematics constraints. For the upper limbs, the end-effectors of the arms are in a free space, and their kinematics constraints primarily include the joint range and the number of DOF. For the lower limbs, since the contact conditions between the feet and the ground are the key factors for humanoid locomotion, the kinematics constraints of low limbs must include the ground contact conditions in addition.

The purpose of dynamics mapping is to make humanoid motion satisfy constraints such as dynamic stability and the actuator's properties, because the mass distribution and the actuator power of the humanoid model are different from those of the human actor.

Through the kinematics mapping and dynamics mapping, the obtained humanoid motion may be a little different from the human actor's motion. Moreover, the actor's motion is a teaching motion, and it is therefore expected to keep the similarity of the human actor's motion, satisfying the kinematics and dynamics constraints.

3. Kinematics Constraints and Dynamic Stability

3.1. *Kinematics constraints*

The kinematics constraints include joint angle range, workspace, and limb contact. For example, the joint angle must be within its range:

$$q_{ri\,\min} \leq q_{ri} \leq q_{ri\,\max}, \tag{1}$$

where $i = 1, 2, \ldots n, n$ is the total number of DOF, q_{ri} denotes the angle of each joint and $(q_{ri\,\min}, q_{ri\,\max})$ denotes the joint angle limitation. The contact constraints between the humanoid feet and the ground are crucial for humanoid locomotion. Since the length of the leg limbs is not in proportion to the bones of the human actor, the ground constraints may not be satisfied, which may result in trampling, slumping, and glissading.

When the humanoid robot moves from the single-support phase, the swing foot should land on the ground with the designed position and orientation. In the case of trampling

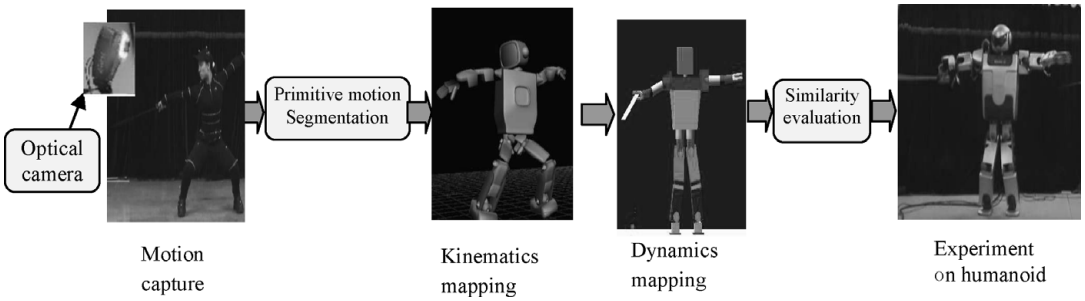

Fig. 2. Procedure of motion generation.

https://doi.org/10.1017/S0263574709990439 Published online by Cambridge University Press

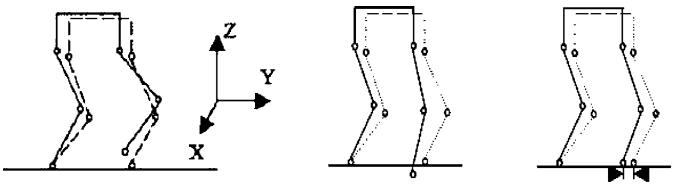

(a) Trampling out (b) Slumping (c) Glissading

Fig. 3. Ground contact constraints.

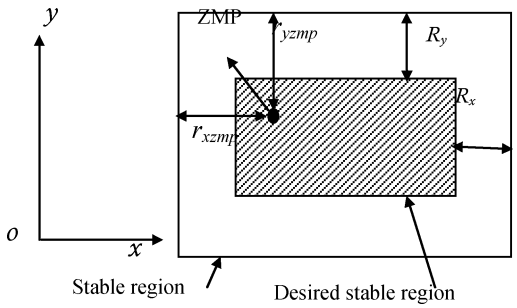

Fig. 4. Stable region and stability margin.

(Fig. 3a), the foot is in the air. Conversely, the foot is under the ground surface in the case of slumping (Fig. 3b). Both cases cannot be applied to humanoid motion.

During the double-support phase, both feet should be stationary on the ground with no slip between the feet and the ground. However, the positions of one or both feet may change; that is, the glissade (Fig. 3c) occurs when the actor's angle data is applied directly to the humanoid robot. To keep the designed contact position and orientation between the feet and the ground, the kinematics constraint can be given as follows:

$$\begin{cases} d_{\min} \neq 0 \\ d_{\min} = \min\{((x_j - x_k)^2 + (y_j - y_k)^2 + (z_j - z_k)^2)^{1/2}\} \end{cases}, \tag{2}$$

where (x_j, y_j, z_j) and (x_k, y_k, z_k) represent two arbitrary points in different limbs of humanoid robot, $d_{\min}$ is the safe distance for collision free between two points on the limbs and truck. Equation (3) is the ground contact constraints:

$$P_R - P_L = F_r(\theta_r), \tag{3}$$

where P_R and P_L denote the designed position vectors of the right foot and the left foot of the humanoid respectively, $P_{\mathrm{R}} = [x_{rf}, y_{rf}, z_{rf}, q_{rx}, q_{ry}, q_{rz}]^T$, $P_L = [x_{lf}, y_{l_f}, z_{lf}, q_{lx}, q_{ly}, q_{lz}]^T$, (x_{rf}, y_{rf}, z_{rf}), and (x_{lf}, y_{lf}, z_{lf}) are the Cartesian coordinate of right foot and left foot, (q_{rx}, q_{ry}, z_{rz}) and (q_{lx}, y_{ly}, z_{lz}) are the attitude angles of right foot and left foot relative to x-axis, y-axis, and z-axis. $F_r(\theta_r)$ denotes the kinematics function and θ_r represents the joint angles on the two legs.

3.2. Stability criterion

We use the zero moment point (ZMP) criterion introduced by Vukobratovic to adjust the stability of the humanoid motion.[1] The ZMP can be computed by the following equations:

$$x_{\mathrm{zmp}} = \frac{\sum_{i=1}^{N} m_i(\ddot{z}_i + g)x_i - \sum_{i=1}^{N} m_i \ddot{x}_i z_i - \sum_{i=1}^{N} I_{iy}\ddot{\Omega}_{iy}}{\sum_{i=1}^{N} m_i(\ddot{z}_i + g)}, \tag{4}$$

$$y_{\mathrm{zmp}} = \frac{\sum_{i=1}^{N} m_i(\ddot{z}_i + g)y_i - \sum_{i=1}^{N} m_i \ddot{y}_i z_i - \sum_{i=1}^{N} I_{ix}\ddot{\Omega}_{ix}}{\sum_{i=1}^{N} m_i(\ddot{z}_i + g)}, \tag{5}$$

where $(x_{\mathrm{zmp}}, y_{\mathrm{zmp}}, 0)$ is the coordinate of the ZMP, N is the number of links, m_i is the mass of link i, g is the gravitational acceleration, and (x_i, y_i, z_i) is the coordinate of the mass center of link i on the absolute Cartesian coordinate system, I_{ix} and I_{iy} are the inertial components, $\ddot{\Omega}_{ix}$ and $\ddot{\Omega}_{iy}$ are the absolute angular velocity components around x-axis and y-axis at the center of gravity of link i.

The convex hull of the contact points between the feet and the ground is defined as stable region. If the ZMP is within the stable region, the robot is able to walk stably. The minimum distance between the ZMP and the boundary of the stable region is called the stability margin (Fig. 4). If the stability margin is larger, the robot will walk in a more stable manner. Therefore, in order to ensure that the stability margin is enough for the robot, the ZMP should be kept within a region called the desired stable region where the stability margin of the ZMP is larger than a specified value. The desired stable region Ω is denoted by the following equation:

$$\Omega = \{(r_{x\mathrm{zmp}}, r_{y\mathrm{zmp}}) | r_{x\mathrm{zmp}} \geq R_x, r_{y\mathrm{zmp}} \geq R_y, R_x > 0, R_y > 0\}, \tag{6}$$

where $r_{x\mathrm{zmp}}$ and $r_{y\mathrm{zmp}}$ are the stability margin in x direction and y direction, R_x and R_y are the specified minimum stability margin, respectively.

4. Similarity Evaluation

The data obtained from the kinematics mapping needs to be modified to satisfy the dynamic stability and allow the robot to move in a stable manner. Further more, it is expected that the humanoid movements are highly similar to those of the human actor.

As mentioned above, many researchers discussed how to obtain humanoid motion based on human motion capture. However, how to evaluate the similarity of the humanoid motion comparing with the human motion quantitatively has not been studied sufficiently. In addition, most of previous published methods on similarity concern the movements at some fixed time,[11,13,15,16,18–24] and the rhythm of the performance has rarely been studied.

Actually, the human actor's performance is rhythmic. The humanoid robot motion should have similar rhythm of the human actor. Hence the evaluation of the humanoid robot motion should not only include the spatial similarity, but

https://doi.org/10.1017/S0263574709990439 Published online by Cambridge University Press

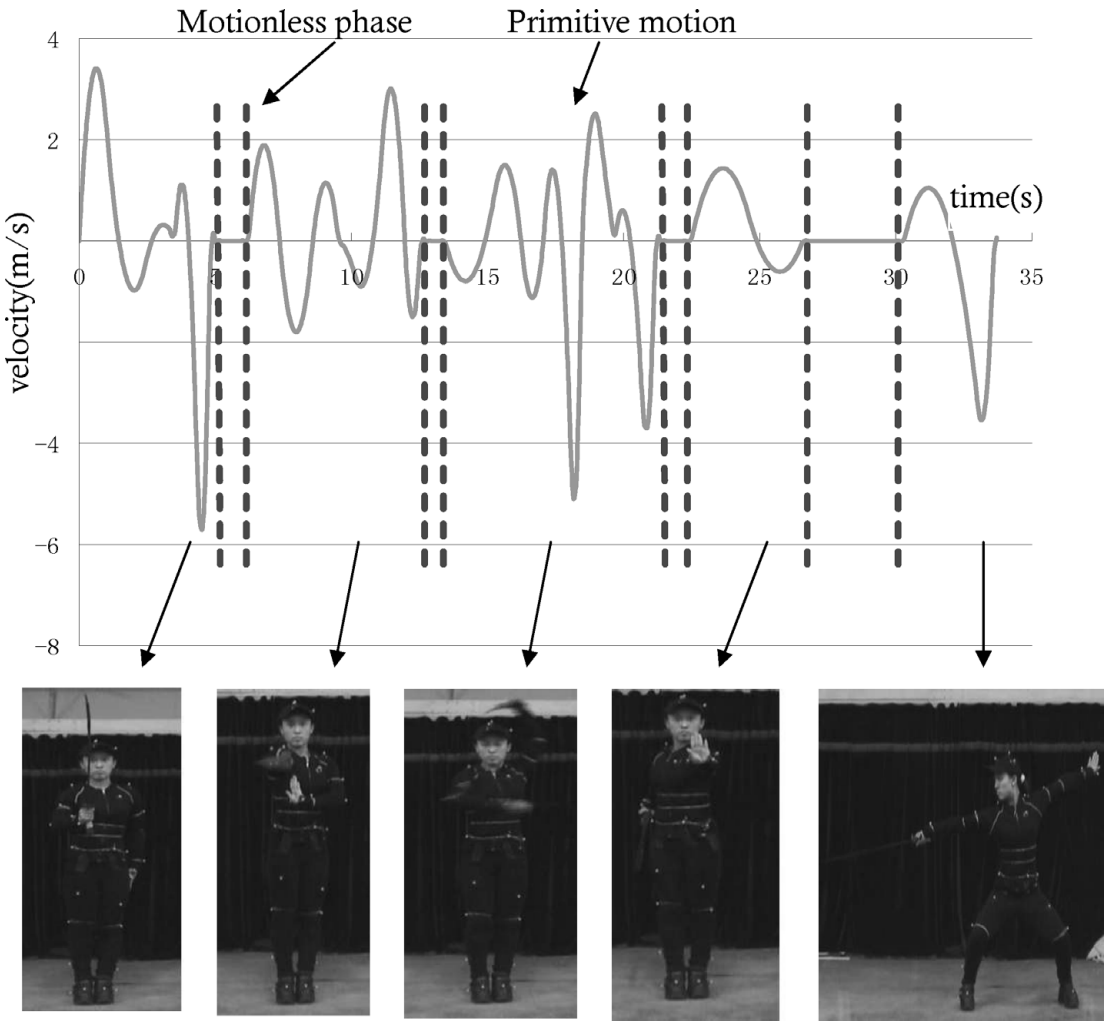

Fig. 5. Segmentation result of hand movement.

also include the temporal similarity of rhythm with the human motion. This section discusses the evaluation function considering the spatial and the temporal similarity.

4.1. Segmentation of primitive motion

We divide the motion into two types, motionless phase and primitive motion. The motionless phase is when the actor takes a static pose for a moment and the motion speed is zero at that time. The transition between two motionless phases is regarded as a primitive motion. That is to say that any two near primitive motions are separated by one motionless phase. From this viewpoint, each primitive motion is independent. It is possible that different parts of the body perform primitive motions, which are independent from each other in their own timing. We consider that synchronized primitive motions of some parts can be integrated into one primitive. Note that the motion segmentation of arm and leg is different. Leg motion involves contact conditions between the foot and the ground, so we consider the arm motion and leg motion separately. In this paper, the target motion of humanoid robot is Chinese Kungfu "Sword" which requires high speed and high stability. The segmentation result of hand movement according to the speed trajectory is shown in Fig. 5.

4.2. Similarity function

The spatial similarity between the human and the humanoid can be expressed in two ways: the relations of the positions of the end-effectors and the trajectories of joint angles between the humanoid robot and the human actor. Since the limb length of the humanoid model differs from that of the human actor, the end-effectors' position of the humanoid may be considerably different from the human actor's. When we use the relations of the positions of the end-effectors to evaluate the similarity, we should take the length of the limbs into consideration. In this case, the joint angles can be acquired by inverse kinematics. Since the actor's joint angles have been obtained, the relations of the trajectories of joint angles are used to evaluate the similarity.

The rhythm similarity can be expressed by the relation of the velocity between the humanoid robot and the human actor. The velocity changes according to the rhythm.

Let $j(j = 1, 2, \ldots, m)$ be the number of the sequence of primitive motion after segmentation. For arbitrary primitive motion j: Let T_j^h be the time taken by human actor, we sampled this primitive motion with time interval $\Delta T^h = \frac{T_j^h}{k}$, and the number of sample points is k. Let T_j^r be the time taken by humanoid robot, we sampled this primitive motion with

https://doi.org/10.1017/S0263574709990439 Published online by Cambridge University Press

time interval $\Delta T^r = \frac{T_j^r}{k}$, and the number of sample points is k.

Since the number of DOF of the human is different from that of the humanoid, we simplified the human motion to make the number of DOF the same as that of the humanoid. The similarity function for arbitrary primitive motion j is defined as follows:

$$S_j = \alpha \cdot \frac{1}{1 + \sum_{i=1}^{n} K_i \cdot \beta_i} + (1 - \alpha) \cdot \frac{1}{1 + \sum_{i=1}^{n} \beta_i'}, \quad (7)$$

where i is the sequence number of the joints, β_i represents the spatial effect on similarity, β_i' represents the temporal effect on similarity, $\beta_i = \frac{\|Q_{ri}(t^r) - Q_{hi}(t^h)\|}{\Delta Q_{ri}(t^r)}$, $\beta_i' = \frac{\|\dot{Q}_{ri}(t^r) - \dot{Q}_{hi}(t^h)\|}{\Delta \dot{Q}_{ri}(t^r)}$; $Q_{ri}(t^r) = [\, q_{ri}(t_1^r)\ q_{ri}(t_2^r) \ldots q_{ri}(t_k^r)\,]^T$ denotes the ith joint angles of the humanoid robot at sample points after kinematics mapping and dynamics mapping, $Q_{hi}(t^h) = [\, q_{hi}(t_1^h)\ q_{hi}(t_2^h) \ldots q_{hi}(t_k^h)\,]^T$ denotes the ith joint angles of the human actor at sample points, $\Delta Q_{ri}(t^r) = |Q_{ri}(t^r)_{\max} - Q_{ri}(t^r)_{\min}|$ denotes the maximum difference of the humanoid ith joint angles at sample points, $\Delta \dot{Q}_{ri}(t^r) = |\dot{Q}_{ri}(t^r)_{\max} - \dot{Q}_{ri}(t^r)_{\min}|$ denotes the maximum difference of the humanoid ith joint velocity at sample points, K_i is the scale coefficient of each joint; S_j is the effect coefficient, and $0 \le \alpha \le 1$. The former part of the function denotes the spatial similarity, and the latter part of the function denotes the temporal similarity. So the function only denotes the temporal similarity, if $\alpha = 1$; the function only denotes the spatial similarity, if $\alpha = 0$. The temporal similarity is important here, because the typical characteristics of Chinese Kungfu "Sword" are speediness, valor, rhythm and harmony. Therefore, we set $\alpha = 0.5$. $0 \le S_j \le 1$, and the larger the value of S_j is, the greater the similarity is. If $S_j = 1$, the similarity of humanoid movements is maximal.

For each primitive motion, we can obtain its similarity value through Eq. (7). This value expresses both the spatial similarity at the sample time and the temporal similarity during the period of the primitive motion. In addition, to imitate the whole human performance in rhythm, the velocity of each primitive motion performed by humanoid should be quicker or slower to the same extent, comparing with the velocity of the same primitive motion performed by human actor:

Take T^h as the duration of the whole performance of the human actor, and let $T^h = \sum T_j^h$. Take T^r as the duration of the whole performance of the humanoid robot, and let $T^r = \sum T_j^r$.

For arbitrary primitive motion j, the following constraint should be satisfied:

$$1 - \varepsilon \le \frac{T_j^h}{T_j^r} \Big/ \frac{T^h}{T^r} \le 1 + \varepsilon, \quad (8)$$

where ε is the threshold, and $\varepsilon > 0$.

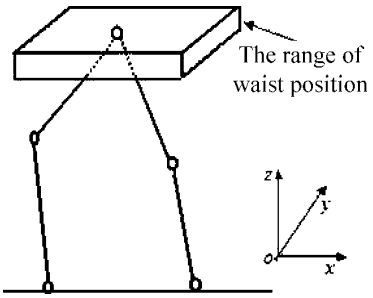

Fig. 6. The adjusting range of waist position.

5. Humanoid Motion

As mentioned above, for each primitive motion, the actor's data should be modified before being adopted by the humanoid. The foot trajectories have been modified during the kinematics mapping, and the foot position has less effect on the stability than the waist position, so only the waist position is modified during the stability adjustment. The modification range of the waist position (Fig. 6) is given as:

$$\begin{cases} x_{w\min} \le x_w \le x_{w\max} \\ y_{w\min} \le y_w \le y_{w\max} \\ z_{w\min} \le z_w \le z_{w\max} \end{cases}, \quad (9)$$

where (x_w, y_w, z_w) is the coordinate of the waist, $(x_{w\min}, x_{w\max})$, $(y_{w\min}, y_{w\max})$, $(z_{w\min}, z_{w\max})$ denote the adjusted ranges in x, y, and z directions. We can get the minimum and maximum ranges in x, y, z directions according to kinematics constraints.

As analyzed above, the humanoid motion with high similarity, satisfying the kinematics constraints and dynamic stability, can be formulated as the following problem:

$$\max S_j, \quad (10)$$

where S_j is the similarity function for the primitive motion j, which is expressed in Eq. (7). To solve Eq. (10), we propose an algorithm shown in Fig. 7. First, kinematics mapping is performed to satisfy the kinematics constraints, and then the waist position is modified to adjust the dynamic stability to satisfy constraint Eq. (6) according to the stability criterion, which is showed in Section 3.2. If it does not satisfy Eq. (6), dynamics mapping should be done again. The next similarity value is calculated by Eq. (7). If the waist position is out of its ranges in x, y, and z directions, we return to perform kinematics mapping again. For the final primitive motion, we select the trajectory that has the highest similarity value. Then the whole performance can be obtained by connecting these primitive motions smoothly, satisfying constraint Eq. (8).

Since the whole performance consists of independent primitive motions, the whole performance performed by humanoid robot will have high similarity if each primitive motion has high similarity.

https://doi.org/10.1017/S0263574709990439 Published online by Cambridge University Press

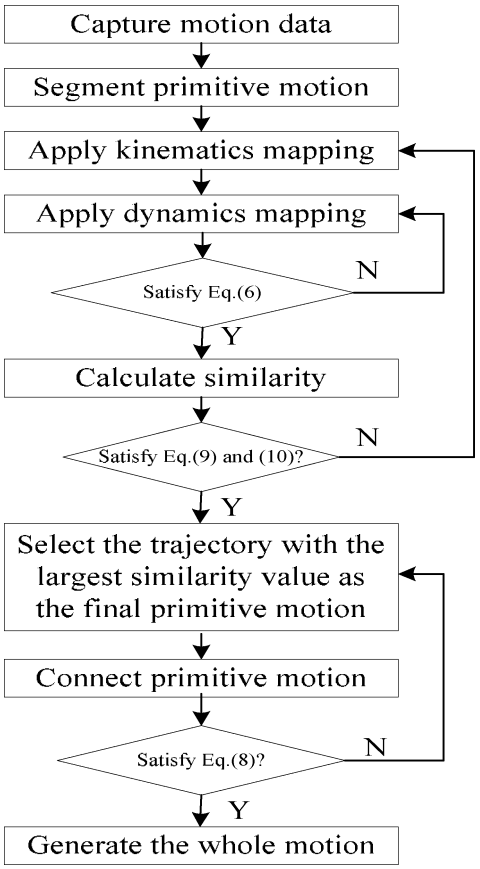

Fig. 7. Algorithm for humanoid motion.

6. Simulation and Experiments

For the experiment, we developed a humanoid robot, BHR-02, with 32 DOF. The parameters of the robot are shown in Table I. Each joint of the robot is actuated by a DC motor with a harmonic-drive reduction gear. Thirty-two DC servomotors are centrally controlled by an industry CPU board with Pentium processors. There are 5 ISA bus expansion boards, including two boards for A/D, D/A and counter, two boards for force sensor, and one board for Ethernet. The OS is RT-Linux.

BHR-02 has sensory devices, including 2 6-axes force/torque sensors, 3 accelerometers, and 3 gyro-sensors. Each of the two force/torque sensors is located on each foot to detect the contact force between the foot and the ground. The accelerometers and the gyro-sensors are located on the body to estimate body acceleration and inclination, relative to the gravitational direction.

We use the proposed method on our developed humanoid BHR-02 to realize the Chinese Kungfu "sword" motion and evaluate its similarity qualitatively and quantitatively. The Kungfu "sword" motion is a complicated and dynamic Chinese Kungfu movement.

Because the "sword" motion is very quick, it's difficult for the humanoid robot to maintain stability. In order to keep the humanoid robot from tipping over, the sensory reflex control is applied on-line.[17]

Figure 8 evaluates the similarity qualitatively. Figure 8(a) shows the sequence of the primitive motions extracted from Chinese Kungfu "sword" performed by the human actor;

Table I. Parameters of humanoid robot.

	Head	Trunk	Arm	Thigh	Crus	Foot
Length (cm)	22	54.1	54	31.5	31.5	13.5
Weight (kg)	1.1	17.2	3.5	5.8	3.9	1.5

Table II. Similarity in each primitive motion.

	Primitive motion 1	Primitive motion 2	Primitive motion 3	Primitive motion 4	Primitive motion 5
S_j	0.963	0.743	0.772	0.685	0.821

Fig. 8(b) shows the corresponding motion performed by the humanoid robot model after kinematics mapping; Fig. 8(c) shows the corresponding motion performed by the humanoid robot model after dynamics mapping; Fig. 8(d) shows the corresponding motion performed by the real humanoid robot. The similarity value of each primitive motion ($j = 1 \sim 5$) is shown in Table II. Figure 9 shows the stability margin of the humanoid robot in x and y directions, without considering the dynamic stability. We can see that the robot will tip over because the ZMP is sometimes outside the stable region. Figure 10 shows the stability margin after dynamics mapping. It is clear that, after considering the dynamic stability, the ZMP is almost in the center of the stability region. For quantitative similarity evaluation, we present a figure of hip joint angle as an example. Figure 11 shows the trajectories of hip joint before and after kinematics mapping and dynamics mapping. We can see that the trajectory is smoother, and the joint angle is within the angle range, after kinematics mapping and dynamics mapping.

We take the trajectory which has the highest similarity as the final trajectory for each primitive motion, on the condition that the trajectory satisfies the kinematics constraints and dynamic stability. In some cases, similarity values are small, for example, primitive motion 4 as shown in Table II, because the motion range of the human "sword" is very large. Moreover, the joint angle ranges of the humanoid robot are limited, due to the mechanism's structural limitation. In order to satisfy the dynamics constraints of the humanoid robot, major adaptations have been performed in some key frames, so the motions of the humanoid robot in these frames are considerably different from those of the human actor. The similarity of primitive motion 1 is nearly 1, because the velocity is slow and the movement range is small.

7. Conclusions

In this paper, we focus on the design and similarity evaluation on complicated humanoid motion. The main results of this paper can be summarized as follows:

(i) Similarity function to evaluate similarity quantitatively including spatial and temporal factors is formulated, and the algorithm to obtain the humanoid motion with high similarity, and satisfying the kinematics constraints and dynamic stability, is presented.

https://doi.org/10.1017/S0263574709990439 Published online by Cambridge University Press

(a) Primitive motions extracted from Chinese Kungfu "sword" performed by the human actor

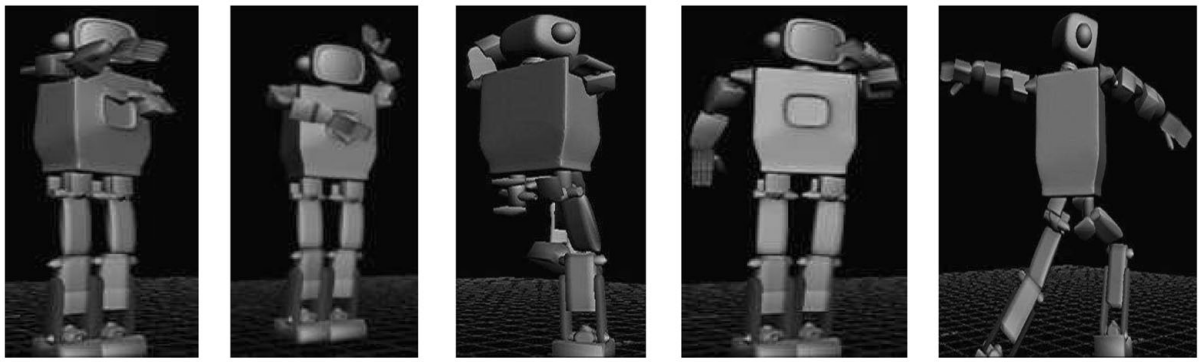

(b) Corresponding motion performed by the humanoid robot model after kinematics mapping

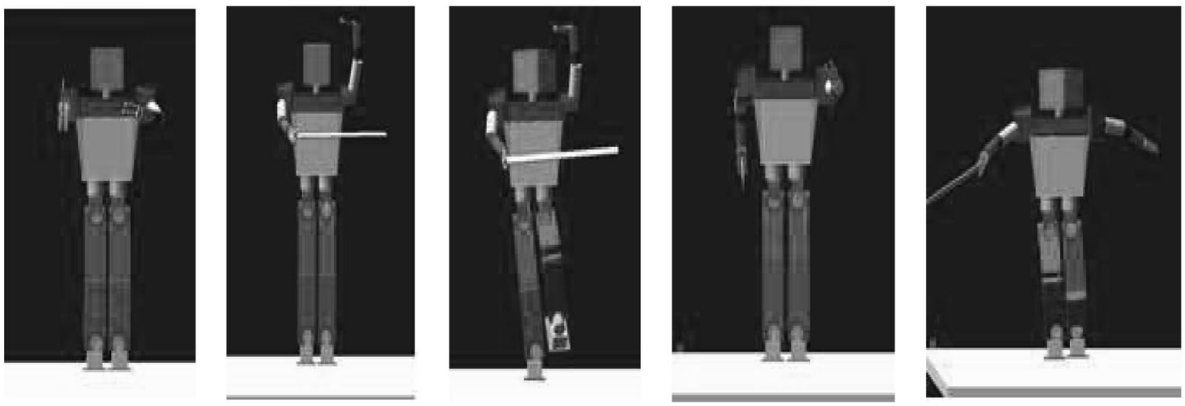

(c) Corresponding motion performed by the humanoid robot model after dynamics mapping

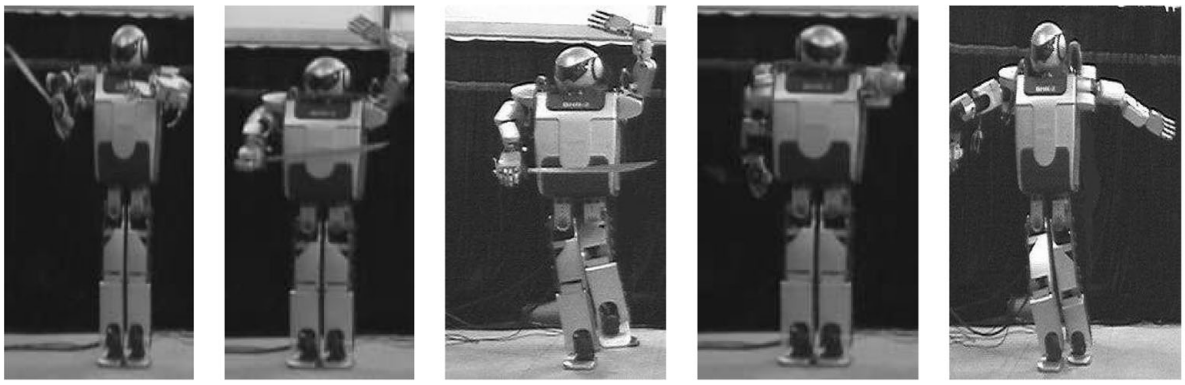

(d) Corresponding motion performed by the humanoid robot

Fig. 8. Primitive motions of human actor and humanoid.

https://doi.org/10.1017/S0263574709990439 Published online by Cambridge University Press

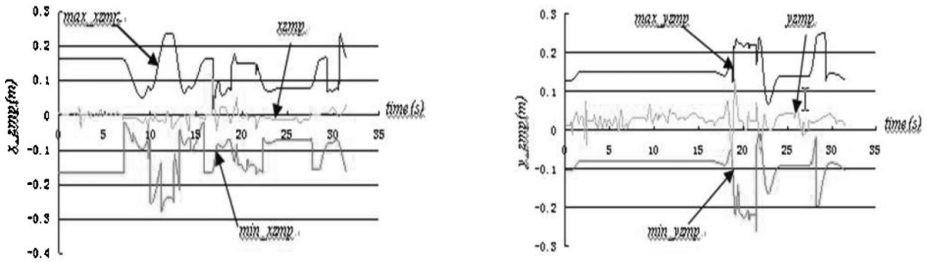

(a) Stability margin in x direction (b) Stability margin in y direction

Fig. 9. Stability margin without considering dynamic stability.

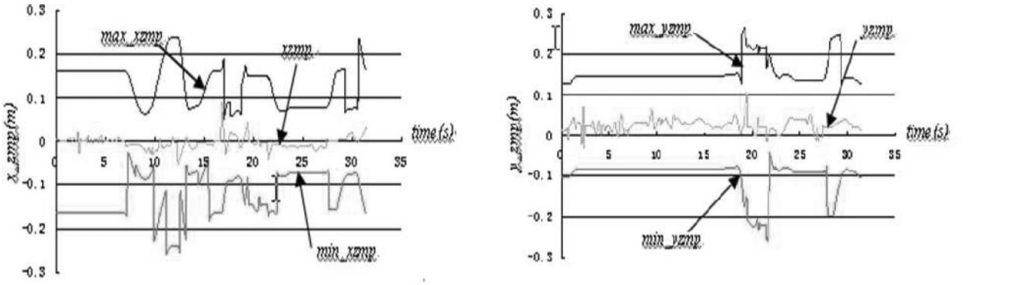

(a) Stability margin in x direction (b) Stability margin in y direction

Fig. 10. Stability margin after considering dynamic stability.

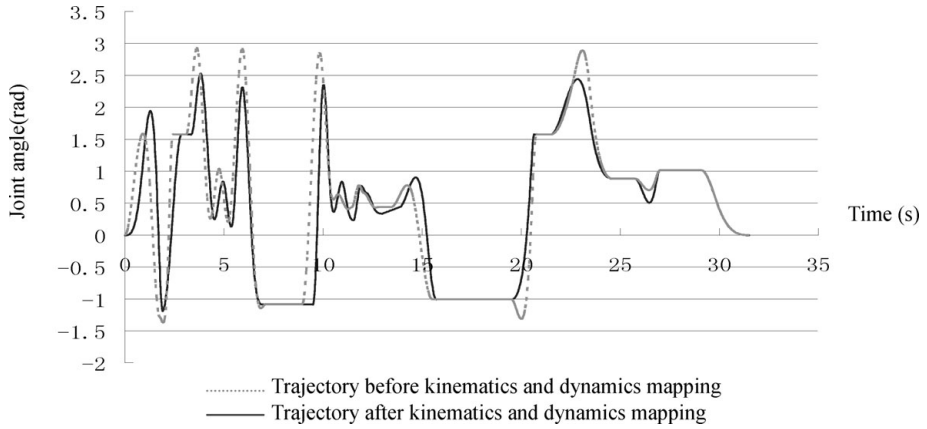

Fig. 11. Trajectories of humanoid hip joint.

(ii) The method of complicated dynamic motion trajectory generation on the basis of human motion is proposed, and the kinematics constraints and dynamic stability are studied.
(iii) The effectiveness of our proposed method is illustrated through "sword" experiment using our developed humanoid robot.

For some complex motions which are difficult for the humanoid to perform due to the constraints, such as the motor torque and mechanism, the similarity value of some primitive motions may be low. In such a case the similarity extent of the whole performance is relevant to the complexity of motions and the similarity of primitive motions. This issue will be studied in our future work.

Acknowledgments

This work was supported by National High Technology Research and Development Program under Grant 2008AA042601, National Natural Science Foundation of China under Grant 60874048, and 111 Project under Grant B08043.

References

1. M. Vukobratovic and D. Juricic, "Contribution to the synthesis of biped gait," *IEEE Trans. Bio-Med. Eng.* **BME-16**(1), 1–6 (1969).
2. J. K. Hodgins and M. H. Raibert, "Adjusting step length for rough terrain locomotion," *IEEE Trans. Robot. Autom.* **7**, 289–298 (1991).

https://doi.org/10.1017/S0263574709990439 Published online by Cambridge University Press

3. Q. Huang, K. Yokoi, S. Kajita, K. Kaneko, H. Arai, N. Koyachi and K. Tanie, "Planning walking patterns for a biped robot," *IEEE Trans. Robot. Autom.* (2001) pp. 280–289.
4. J. Yamaguchi, E. Soga, S. Inoue and A. Takanishi, "Development of a Biped Humanoid Robot Control Method of Whole Body Cooperative Dynamic Biped Walking," *Proceeding of IEEE International Conference on Robotics and Automation*, Detroit, Michigan (1999) pp. 368–374.
5. A. Takanishi, M. Tochizawa, H. Karaki and I. Kato, "Dynamic Biped Walking Stabilized with Optimal Trunk and Waist Motion," *Proceeding of IEEE International Workshop on Intelligent Robotics and Systems*, Tsukuba, Japan (1989) pp. 187–192.
6. K. Hirai, M. Hirose, Y. Haikawa and T. Takenaka, "The Development of Honda Humanoid Robot," *Proceeding of IEEE International Conference on Robotics and Automation*, Leuven, Belgium (1998) pp. 1321–1326.
7. Q. Huang, S. Kajita, N. Koyachi, K. Kaneko, K. Yokoi, H. Arai, K. Komoriya and K. Tanie, "A High Stability, Smooth Walking Pattern for a Biped Robots," *Proceeding of IEEE International Conference on Robotics and Automation*, Detroit, Michigan (1999) pp. 65–71.
8. F. Gubina, H. Hemami and R. B. McGhee, "On the dynamic stability of biped locomotion," *IEEE Trans. Bio-Med. Eng*. **BME-21**(2), 102–108 (1974).
9. C. L. Shih, Y. Z. Li, S. Churng, T. T. Lee and W. A. Cruver, "Trajectory Synthesis and Physical Admissibility for a Biped Robot During the Single Support Phase," *Proceeding of IEEE International Conference on Robotics and Automation*, Los Alamitos, CA (1990) pp. 1646–1652.
10. S. Kajita, A. Kobayashi and T. Yamamura, "Dynamic walking control of a biped robot along a potential energy conservation orbit," *IEEE Trans. Robot. Autom.* **8**, 431–438 (1992).
11. S. Pollard, J. Hodgins, M. J. Riley and C. Atkeson, "Adapting Human Motion for the Control of a Humanoid Robot," *Proceedings of IEEE International Conference on Robotics and Automation*, Washington, DC (2002) pp. 1390–1397.
12. K. Yamane and Y. Nakamura, "Dynamics Filter—Concept and Implementation of On-Line Motion Generator for Human Figures," *Proceeding of IEEE International Conference on Robotics and Automation*, San Francisco, CA (2000) pp. 688–695.
13. S. Nakaoka, A. Nakazawa, K. Yokoi, H. Hirukawa and K. Ikeuchi, "Generating Whole Body Motion for a Biped Humanoid Robot from Captured Human Dances," *Proceeding of IEEE International Conference on Robotics and Automation*, Taipei, Taiwan (2003) pp. 3905–3910.
14. S. Nakaoka, A. Nakazawa, K. Yokoi and K. Ikeuchi, "Leg Motion Primitives for a Dancing Humanoid Robot," *Proceeding of IEEE International Conference on Robotics and Automation*, New Orleans, LA (2004) pp. 610–615.
15. A. Nakazawa, S. Nakaoka, K. Ikeuchi and K. Yokoi, "Imitating Human Dance Motions Through Motions Structure Analysis," *Proceeding of IEEE International Conference on Intelligent Robots and System*, Lausanne, Switzerland (2002) pp. 2539–2544.
16. A. Nakazawa, S. Nakaoka and K. Ikeuchi, "Synthesize Stylistic Human Motion from Examples," *Proceeding of IEEE International Conference on Robotics and Automation*, Taipei, Taiwan (2003) pp. 14–19.
17. D. Kulic, W. Takano and Y. Nakamura, "Combining Automated On-Line Segmentation and Incremental Clustering for Whole Body Motions," *Proceeding of IEEE International Conference on Robotics and Automation*, Pasadena, CA (2008) pp. 2591–2598.
18. G. Wang, Q. Huang, J. Geng, H. deng and K. Li, "Cooperation of Dynamic Patterns and Sensory Reflex for Humanoid Walking," *Proceeding of IEEE International Conference on Robotics and Automation*, Taipei, Taiwan (2003) pp. 2472–2477.
19. S. Kajita, O. Matsumoto and M. Saigo, "Real-Time 3D Walking Pattern Generation for a Biped Robot with Telescopic Legs," *Proceeding of IEEE International Conference on Robotics and Automation*, Seoul, Korea (2001) pp. 2299–2036.
20. H. Lim, Y. Kaneshiharu and A. Takanishi, "Online Walking Pattern Generation for Biped Humanoid Robot with Trunk," *Proceeding of IEEE International Conference on Robotics and Automation*, Washington, DC (2002) pp. 3111–3116.
21. T. Sugihara, Y. Nakamura and H. Inoue, "Real-Time Humanoid Motion Generation Through ZMP Manipulation Based on Inverted Pendulum Control," *Proceeding of IEEE International Conference on Robotics and Automation*, Washington, DC (2002) pp. 1404–1409.
22. K. Nishiwaki, S. Kagami, J. Fuffner, M. Inba and H. Inoue, "Online Humanoid Walking Control System and a Moving Goal Tracking Experiment," *Proceeding of IEEE International Conference on Robotics and Automation*, Taipei, Taiwan (2003) pp. 911–916.
23. S. Setiawan, S. Hyon, J. Yamaguchi and A. Takanishi, "Physical Interaction Between Human and a Bipedal Humanoid Robot-Realization of Human-Follow Walking," *Proceeding of IEEE International Conference on Robotics and Automation*, Detroit, Michigan (1999) pp. 361–367.
24. Q. Huang, Z. Peng, W. Zhang and L. Zhang, "Design of Humanoid Complicated Dynamic Motion Based on Human Motion Capture," *Proceeding of 2005 IEEE/RSJ International Conference on Intelligent Robots and Systems*, Edmonton, AB, Canada (2005) pp. 686–691.

https://doi.org/10.1017/S0263574709990439 Published online by Cambridge University Press